

Discovering Relational Covariance Structures for Explaining Multiple Time Series

Anh Tong and Jaesik Choi

Ulsan National Institute of Science and Technology
50 UNIST-gil, Ulsan, South Korea, 44919

Abstract

Analyzing time series data is important to predict future events and changes in finance, manufacturing, and administrative decisions. In time series analysis, Gaussian Process (GP) regression methods recently demonstrate competitive performance by decomposing temporal covariance structures. The covariance structure decomposition allows exploiting shared parameters over a set of multiple, selected time series. In this paper, we present two novel GP models which naturally handle multiple time series by placing an Indian Buffet Process (IBP) prior on the presence of *shared* kernels. We also investigate the well-definedness of the models when infinite latent components are introduced. We present a pragmatic search algorithm which explores a larger structure space efficiently than the existing search algorithm. Experiments are conducted on both synthetic data sets and real-world data sets, showing improved results in term of structure discoveries and predictive performances. We further provide a promising application generating comparison reports from our model results.

Introduction

Time series data analysis is important for numerous real-world applications: signal processing of audio and video data; the study of financial variables such as stocks, currencies, and crude oil prices. When several data sources are correlated, a model considering more observations can lead to more accurate prediction. Let us take stock trading as an example. Traders never make a decision solely based on observing an attribute of stock. They usually consider the relations among a group of stocks e.g. a stock can affect one or many other stocks. Thus, it is critical to learn how multiple time series are correlated. Moreover, it is non-trivial to extract important relations among multiple time series. In the perspective of making sense of data, there are numerous practical applications in visualizing, filtering or reporting about these time series based on their inherent relations.

Beyond classical regression methods like ARMA, ARIMA, and their extensions (F. Engle 1982; Bollerslev 1986; Box and Reinsel 1976; Hamilton 1994), a nonparameteric regression based on Gaussian Process (GP) (Rasmussen and Williams 2005) contributed a highly general framework called Automatic Bayesian Covariance Discovery (ABCD) (Duve-

naud et al. 2013; Lloyd et al. 2014; Ghahramani 2015). The ABCD automatically extracts an appropriate compositional covariance structure to fit data based on grammar rules; generate human-friendly reports explaining data. Previously, selecting GP kernels was heavily based on expert knowledge or trial-and-error. The compositional covariance structure makes the GP models more expressive and interpretable so that GP kernels are explained in a form of natural language. There are cognitive studies (Schulz et al. 2016; 2017) showing that compositional functions are intuitively preferred by human; some attempts to scale up or improve the model selection in ABCD (Kim and Teh 2018; Malkomes, Schaff, and Garnett 2016). Exploiting these key properties of compositional kernel, we develop a kernel composition framework for multiple time series which produces explainable outputs with an improved predictive accuracy.

Multi-task GP regression methods have established a solid foundation in (Bonilla, Chai, and Williams 2007; Titsias and Lázaro-Gredilla 2011; Álvarez, Rosasco, and Lawrence 2012; Wilson, Knowles, and Ghahramani 2012; Guarnizo, Álvarez, and Orozco 2015)¹. However, assigning compositional kernel structures is not investigated in the existing multi-task GP regression methods. Notably, the multi-output GP regression network (GPRN) (Wilson, Knowles, and Ghahramani 2012) is highly general, and models data by the combinations of latent GP functions and weights which are also GPs. Applying structure search is challenging due to the huge search space to cover the whole network. There is an existing method which takes into account compositional kernels in multiple sequences but assumes a simple, naive global structure (Hwang, Tong, and Choi 2016). Thus, such a method is not applicable to analyze many, heterogeneous time series, accurately. In order to select appropriate covariance structures for multiple correlated sequences, we model time series by additive structures which are, instead of staying fixed, searched over a set of kernels. We place Indian Buffet Process (IBP) (Griffiths and Ghahramani 2005; 2011) prior over a indicator matrix that represents whether they are shared one or many of these additive kernels. We introduce a search algorithm enables us to explore a larger kernel space.

We also present two novel models to handle heterogeneous

¹More details of related work are discussed in Appendix

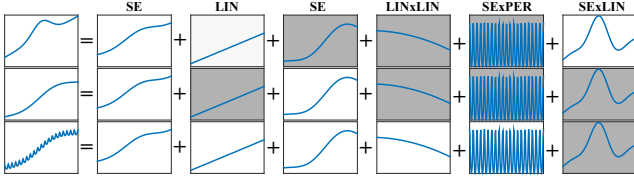


Figure 1: A simple explanation of our model, gpLFM. The first column shows three time series. They are decomposed into shared components (remaining columns). The white/gray colors in the background indicate the active/inactive components. Note that the plots have different scales on the vertical axis.

but correlated multiple time series. The first model uses IBP matrix to select GP realizations as features. The second model generates GP kernels to fit data from a stochastic kernel process where IBP is placed over a kernel space. We respectively call these two models as Latent GP Feature Model (gpLFM) and Latent Kernel Model (LKM). This paper offers the following contributions: (1) we introduce our proposed models, justify their well-definedness and develop their approximate inference algorithms; (2) we introduce a search procedure applying for multiple time series and our working models; (3) an application making comparison reports among multiple time series.

This paper is structured as follows. Section presents our proposed models: gpLFM and LKM. Section introduces a search procedure working with the two models. Section shows our experiments on several real-world data sets and give comparison report produced from our models. We conclude in Section .

Preliminary

In this section, we provide a brief review of the Automatic Bayesian Covariance Discovery (ABCD) framework (Grosse et al. 2012; Duvenaud et al. 2013; Lloyd et al. 2014; Ghahramani 2015) and Indian Buffet Process (IBP) (Griffiths and Ghahramani 2005).

The ABCD framework The ABCD framework follows a typical Bayesian modeling process (see (MacKay 2002, Ch. 28, p. 346)), being composed of several parts e.g. a language of models, a search procedure among models, and a model evaluation. The framework makes use of Gaussian Process (GP) (Rasmussen and Williams 2005) to perform various regression tasks.

Selecting kernel functions plays a crucial role in learning GP. ABCD searches a model out of an open-ended language of models which is constituted from a context-free grammar and base kernels. The base kernels reveal the high-level properties of data. They consist of white noise (WN), constant (C), squared exponential (SE), periodic (PER), change-point (CP), and change-window (CW)(see Appendix). The grammar makes it possible to explore and generate new kernels from base ones via composition rules such as the product rule and the sum rule. A greedy search is applied in ABCD like

in (Grosse et al. 2012), picking the most appropriate model based on a criterion e.g. Bayesian Information Criteria (BIC). Once the search procedure is finished, a human-readable report is generated from the interpretability of GP base kernels and their compositions.

Indian Buffet Process The IBP is a nonparametric process in (Griffiths and Ghahramani 2005) discovers latent features among a set of objects. This nonparametric process defines a distribution over a binary matrix \mathbf{Z} with finite rows and infinite columns. The matrix indicates feature assignments where the element at the i -th row and the j -th column expresses the presence or absence of the j -th feature in the i -th object. One of the typical applications of IBP is the linear-Gaussian latent feature model (LFM) (Griffiths and Ghahramani 2005). Data represented by \mathbf{X} is factorized into an IBP latent matrix \mathbf{Z} multiplying with a feature matrix \mathbf{A} with a Gaussian noise matrix \mathcal{E} ,

$$\mathbf{X} = \mathbf{Z}\mathbf{A} + \mathcal{E}. \quad (1)$$

Models

In this section, we present our models: Latent GP Feature Model (gpLFM) and Latent Kernel Model (LKM). Along with each model, we give a variational inference algorithm. We provide qualitative comparisons of gpLFM, LKM and a related model (R-ABCD (Hwang, Tong, and Choi 2016)). We then discuss on the well-definedness of gpLFM and LKM when using a nonparametric prior.

Problem setting and notation Given N time series, each time series has D data points. Let us denote $\mathbf{x}_n = (x_{n1}, \dots, x_{nD})^\top$ be a vector representing the n -th time series where x_{nd} is the data point of the n -th time series at the d -th time step t_d . To clarify further notation, we denote a data matrix \mathbf{X} taking \mathbf{x}_n s as rows. We latter introduce a latent matrix \mathbf{Z} taking \mathbf{z}_n s as rows and a feature matrix \mathbf{F} taking \mathbf{f}_k as rows.

Latent GP Feature Model

Latent GP Feature Model (gpLFM) aims to decompose \mathbf{x}_n into additive features in which each of them is sampled from a GP

$$\mathbf{x}_n = \sum_{k=1}^K z_{nk} \mathbf{f}_k + \epsilon_n, \quad (2)$$

where $z_{nk} \in \{0, 1\}$ is the element of $N \times K$ matrix \mathbf{Z} indicating whether time series \mathbf{x}_n has component \mathbf{f}_k ; ϵ_n is a vector having each element independently follows a Gaussian noise $\mathcal{N}(0, \sigma_n^2 \mathbf{I})$; for any $k = 1 \dots K$, \mathbf{f}_k is a GP with a covariance kernel \mathbf{C}_k , denoted as $\mathbf{f}_k \sim \mathcal{GP}(\mathbf{0}, \mathbf{C}_k)$. Here we use the GP notation for \mathbf{f}_k which is a realization of a GP. When stacking \mathbf{f}_k into a $K \times D$ matrix \mathbf{F} , our model described in (2) can be written as

$$\mathbf{X} = \mathbf{Z}\mathbf{F} + \mathcal{E}, \quad (3)$$

where \mathbf{Z} has a finite number of rows and an unbounded number of columns. The latent features \mathbf{f}_k are shared among a set of time series $\{\mathbf{x}_n | z_{nk} = 1\}$. We place the IBP prior on \mathbf{Z} .

Although our model represented in (3) looks similar to linear-Gaussian model in (1), the correlation among elements in the k -th row of \mathbf{F} described by \mathbf{C}_k distinguishes our model from linear-Gaussian model since there is no correlation between among elements in \mathbf{A} . Figure 1 is an illustrative explanation for gpLFM.

Variational inference for gpLFM We have a generative process for the data and latent variables

$$\mathbf{Z} \sim \text{IBP}(\alpha), \mathbf{f}_k \sim \mathcal{GP}(\mathbf{0}, \mathbf{C}_k), \mathbf{x}_n \sim \mathcal{N}(\mathbf{z}_n^\top \mathbf{F}, \sigma_n^2 \mathbf{I}), \quad (4)$$

where $k \in \{1, \dots, K\}$, $n \in \{1, \dots, N\}$, and α is the concentration parameter. For simplicity, we use $\mathbf{Z} \sim \text{IBP}(\alpha)$ instead of explicit generative processes including (1) sample feature probabilities π_{nk} using a Beta prior with finite case or a stick-breaking prior with infinite case; (2) then, sample z_{nk} from a Bernoulli distribution parameterized by π_{nk} (Doshi et al. 2009). Variational inference method approximates the true posterior $p(\mathbf{Z}, \mathbf{F}|\mathbf{X})$ by an variational distribution $q(\mathbf{Z}, \mathbf{F})$. The method converts the optimization problem of KL divergence between p and q into an equivalent problem by maximizing the evidence lower bound (ELBO) \mathcal{L} ,

$$\begin{aligned} \log p(\mathbf{X}) &= \mathbb{E}_{\mathbf{Z}, \mathbf{F}}[\log p(\mathbf{X}, \mathbf{Z}, \mathbf{F})] + H[q] + \text{KL}(q||p) \\ &\geq \mathbb{E}_{\mathbf{Z}, \mathbf{F}}[\log p(\mathbf{X}, \mathbf{Z}, \mathbf{F})] + H[q] \triangleq \mathcal{L}, \end{aligned}$$

where \mathbb{E} with subscripts indicates the expectation over the approximate posterior distribution, and $H[q]$ is the entropy of q . The joint distribution $p(\mathbf{X}, \mathbf{Z}, \mathbf{F})$ is in the form of $p(\mathbf{Z})p(\mathbf{F})p(\mathbf{X}|\mathbf{Z}, \mathbf{F})$. We apply the mean-field variation inference, factorizing $q(\mathbf{Z}, \mathbf{F}) = q(\mathbf{Z})q(\mathbf{F})$. The $q(\mathbf{Z})$ is further broken down into smaller components $q(z_{nk}) = \text{Bernoulli}(z_{nk}; \nu_{nk})$. The distribution over the feature matrix $p(\mathbf{F})$ is written as $p(\mathbf{F}) = \prod_{k=1}^K p(\mathbf{f}_k)$, approximated by $q(\mathbf{F}) = \prod_{k=1}^K \mathcal{N}(\mathbf{f}_k; \mathbf{m}_k, \mathbf{S}_k)$. With the above specification of the variational distribution, the ELBO \mathcal{L} is

$$\mathcal{L} = \mathbb{E}_{\mathbf{Z}}[\log p(\mathbf{Z})] + \mathbb{E}_{\mathbf{F}}[\log p(\mathbf{F})] + \mathbb{E}_{\mathbf{Z}, \mathbf{F}}[\log p(\mathbf{X}|\mathbf{Z}, \mathbf{F})] + H[q].$$

The detailed formula of ELBO is placed in Appendix . The gpLFM differs from LFM in (Doshi et al. 2009) that it does not allow every element in \mathbf{F} freely follows an independent Gaussian noise as in LFM. Hence, in the maximization step, the variational parameters $\mathbf{m}_k, \mathbf{S}_k$ are updated by

$$\begin{aligned} \mathbf{S}_k &= \left(\mathbf{C}_k^{-1} + \sum_{n=1}^N \frac{\nu_{nk}}{\sigma_n^2} \mathbf{I} \right)^{-1}, \\ \mathbf{m}_k d &= \mathbf{S}_k \left(\sum_{n=1}^N \frac{\nu_{nk}}{\sigma_n^2} \left(\mathbf{x}_n - \sum_{l:l \neq k} \nu_{nl} \mathbf{m}_l \right) \right). \end{aligned} \quad (5)$$

Latent Kernel Model

In the previous section, gpLFM shares feature functions among time series. In this section, we present a new general model which shares kernels instead of functions (fixed realization from kernel). We wish to model each time series with

$$\mathbf{g}_n \sim \mathcal{GP}(\mathbf{0}, \sum_{k=1}^K z_{nk} \mathbf{C}_k), \quad \mathbf{x}_n \sim \mathcal{N}(\mathbf{g}_n, \sigma_n^2 \mathbf{I}),$$

where \mathbf{C}_k are GP kernels. The $p(\mathbf{X}|\mathbf{Z})$ is the product of all $p(\mathbf{x}_n|\mathbf{z}_n)$ where

$$p(\mathbf{x}_n|\mathbf{z}_n) = |2\pi \mathbf{D}(\mathbf{z}_n)|^{-1/2} \exp\left(-\frac{1}{2} \mathbf{x}_n^\top \mathbf{D}(\mathbf{z}_n)^{-1} \mathbf{x}_n\right),$$

with $\mathbf{D}(\mathbf{z}_n) = \sum_{k=1}^K z_{nk} \mathbf{C}_k + \sigma_n^2 \mathbf{I}$. This model focuses on the process of creating the stochastic kernel $\mathbf{D}(\mathbf{z}_n)$ for each \mathbf{x}_n . The kernel selection procedure relies on learning IBP matrix via Bayesian inference. Rather making features as latent variables like in gpLFM, the existence of a kernel in each time series is a hidden variable.

Variational inference for LKM The generative procedure involves

$$\mathbf{Z} \sim \text{IBP}(\alpha), \mathbf{g}_n \sim \mathcal{GP}(\mathbf{0}, \sum_{k=1}^K z_{nk} \mathbf{C}_k), \mathbf{x}_n \sim \mathcal{N}(\mathbf{g}_n, \sigma_n^2 \mathbf{I}).$$

Since the feature \mathbf{F} does not appear in LKM, the mean-field variational inference approximates the posterior $p(\mathbf{Z}|\mathbf{X})$ by $q(\mathbf{Z})$. Here, $q(\mathbf{Z})$ follows the same setup as in gpLFM. By using the aforementioned $p(\mathbf{X}|\mathbf{Z})$ to construct the joint distribution $p(\mathbf{X}, \mathbf{Z}) = p(\mathbf{Z})p(\mathbf{X}|\mathbf{Z})$, we write the ELBO of LKM as

$$\begin{aligned} \log p(\mathbf{X}) &\geq \mathbb{E}_{\mathbf{Z}}[\log p(\mathbf{X}, \mathbf{Z})] + H[q] \\ &= \mathbb{E}_{\mathbf{Z}}[\log p(\mathbf{Z})] + \mathbb{E}_{\mathbf{Z}}[\log p(\mathbf{X}|\mathbf{Z})] + H[q]. \end{aligned}$$

The first term of the lower bound and the entropy $H[q]$ are computed analogously as the variational inference of gpLFM. The evaluation of $\mathbb{E}_{\mathbf{Z}}[\log p(\mathbf{x}_n|\mathbf{z}_n)]$ in $\mathbb{E}_{\mathbf{Z}}[\log p(\mathbf{X}|\mathbf{Z})]$ is expensive since it needs to compute the expectation of the inverse and log-determinant of kernel matrices associated with random variables \mathbf{Z} . Specifically, $\mathbb{E}_{\mathbf{Z}}[\log p(\mathbf{x}_n|\mathbf{z}_n)]$ is written as the summation of $-\frac{1}{2} \mathbf{x}_n^\top \mathbb{E}_{\mathbf{Z}}[\mathbf{D}(\mathbf{z}_n)^{-1}] \mathbf{x}_n$ (or the expectation of data-fit term in GP likelihood) and $-\frac{1}{2} \mathbb{E}_{\mathbf{Z}}[\log |2\pi \mathbf{D}(\mathbf{z}_n)|]$ (or the expectation of GP model complexity). Each of these expectations is the summation of following 2^K terms: (1) $p(\mathbf{z}_n = \mathbf{t}) \mathbf{D}(\mathbf{t})^{-1}$ for all $\mathbf{t} \in \{0, 1\}^K$ in the case of the expectation of inverse matrix; (2) $p(\mathbf{z}_n = \mathbf{t}) \log |2\pi \mathbf{D}(\mathbf{t})|$ for all $\mathbf{t} \in \{0, 1\}^K$ in the case of the expectation of log-determinant. However, it is not practical to estimate an exponential number of inverse or determinant operations. We further bound $\mathbb{E}_{\mathbf{Z}}[\log p(\mathbf{x}_n|\mathbf{z}_n)]$ to make computation tractable.

Expectation of data-fit terms We apply the Jensen's inequality on a convex function $f(\mathbf{A}) = \mathbf{c}^\top \mathbf{A}^{-1} \mathbf{c}$, we have $\mathbf{c}^\top \{\mathbb{E}[\mathbf{A}]\}^{-1} \mathbf{c} \leq \mathbf{c}^\top \mathbb{E}[\mathbf{A}^{-1}] \mathbf{c}$ for any \mathbf{c} (see (Groves and Rothenberg 1969)). In fact, we assign normalized weights w_{nk} for each term in $\left(\sum_{k=1}^K z_{nk} \mathbf{C}_k + \sigma_n^2 \mathbf{I}\right)^{-1}$ to have $(\mathbb{E}[\mathbf{A}])^{-1}$, then we can bound it by

$$\begin{aligned} \mathbf{x}_n^\top &\left(\sum_{k=1}^K w_{nk} \frac{1}{w_{nk}} \left(z_{nk} \mathbf{C}_k + \frac{\sigma_n^2}{K} \mathbf{I} \right) \right)^{-1} \mathbf{x}_n \\ &\leq \mathbf{x}_n^\top \sum_{k=1}^K w_{nk}^2 \left(z_{nk} \mathbf{C}_k + \frac{\sigma_n^2}{K} \mathbf{I} \right)^{-1} \mathbf{x}_n, \end{aligned}$$

where w_{nk} s are all positive, satisfying $\sum_{k=1}^K w_{nk} = 1$.

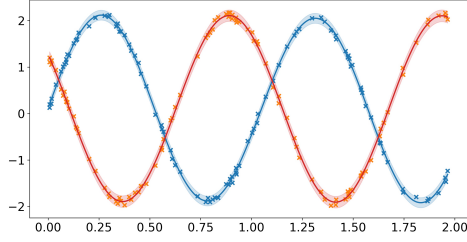


Figure 2: Fitting a toy data using LKM. The toy data set is two realizations from a GP generated from a periodic kernel.

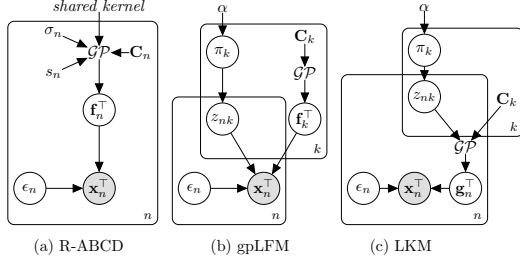


Figure 3: Graphical model of (a) R-ABCD (Hwang, Tong, and Choi 2016), (b) gpLFM, and (c) LKM.

It is important to obtain an appropriate set of weights which affects how tight this bound is, and then creates an objective for learning accurate variational parameters. Naive approaches like using uniform weights is unsuitable. To find w_{nk} , we solve a constraint optimization with an objective in the bound which satisfies that the sum of all weights should be 1. After taking the expectation over \mathbf{Z} , the optimal weights are written as $w_{nk} = a_{nk}^{-1} / \sum_{k=1}^K a_{nk}^{-1}$ with $a_{nk} = \mathbf{x}_n^\top \mathbb{E}_{z_{nk}} \left[(z_{nk} \mathbf{C}_k + (\sigma_n^2 / K) \mathbf{I})^{-1} \right] \mathbf{x}_n$ (explained further in Appendix). Intuitively, the optimal weight w_{nk} is proportional to how much a time series \mathbf{x}_n fits the kernel \mathbf{C}_k where the data-fit term $-\mathbf{x}_n^\top \mathbf{C}_k^{-1} \mathbf{x}_n$ is in the reciprocal way of $\mathbf{x}_n^\top \mathbf{C}_k^{-1} \mathbf{x}_n$ as $(\mathbf{x}_n^\top \mathbf{C}_k^{-1} \mathbf{x}_n)^{-1}$. Now, we can finally bound the expectation of data-fit term as $-\mathbf{x}_n^\top \mathbb{E}_{\mathbf{Z}} [\mathbf{D}(\mathbf{z}_n)^{-1}] \mathbf{x}_n \geq -\sum_{k=1}^K w_{nk}^2 a_{nk}$.

Expectation of model complexity terms Since the log-determinant function is concave, it is straightforward to get lower bound of $-\mathbb{E}_{\mathbf{Z}} [\log |2\pi \mathbf{D}_n|]$ by the log-determinant of the expected matrix as $-\log \left| 2\pi \left(\sum_{k=1}^K \nu_{nk} \mathbf{C}_k + \sigma_n^2 \mathbf{I} \right) \right|$.

Computational advantage As a result of finding the bound of $\mathbb{E}_{\mathbf{Z}} [\log p(\mathbf{x}_n | \mathbf{z}_n)]$, the expectation step is done in linear time, $O(K)$. More specifically, the number of computing matrix inversions and determinants goes down from $O(2^K)$ to $O(K)$ for each computation associated with \mathbf{x}_n .

Comparisons of gpLFM, LKM and R-ABCD

Note that the posterior decomposition of additive Gaussian distributions presents as follows. If $\mathbf{f} = \mathbf{f}_1 + \mathbf{f}_2$, where $\mathbf{f}_1 \sim$

$\mathcal{N}(0, \mathbf{K}_1)$, $\mathbf{f}_2 \sim \mathcal{N}(0, \mathbf{K}_2)$, the conditional distribution of \mathbf{f}_1 given the sum \mathbf{f} is

$$\mathbf{f}_1 | \mathbf{f} \sim \mathcal{N}(\mathbf{K}_1^\top (\mathbf{K}_1 + \mathbf{K}_2)^{-1} \mathbf{f}, \mathbf{K}_1 - \mathbf{K}_1^\top (\mathbf{K}_1 + \mathbf{K}_2)^{-1} \mathbf{K}_1).$$

For the multiple time series setting, each decomposed component under the same Gaussian Process prior could be realized differently in different time series. In other words, for a specific k , $\mathbf{f}_k | \mathbf{x}_n$ would vary when \mathbf{x}_n changes even with the fixed covariance \mathbf{C}_k . A simple setup in Figure 2 can verify this observation. We generate two sequences from a single periodic GP and then run LKM on this data with two different periodic kernels $\mathbf{C}_1, \mathbf{C}_2$. LKM learned $\mathbf{Z} = [0, 1; 0, 1]$ which means that LKM is able to recognize these two realizations from one GP. While gpLFM output $\mathbf{Z} = [1, 0; 0, 1]$, interpreting data as separated features. In addition, the variational inference update of approximating \mathbf{f}_k in gpLFM does not truly stem from GP but is adjusted with other features to fit data using the approximation \mathbf{S}_k of \mathbf{C}_k (see Eq. 5).

In fact, LKM is more general than explicitly decomposing a time series to individual features like in gpLFM or existing work (Titsias and Lázaro-Gredilla 2011; Guarnizo, Álvarez, and Orozco 2015). The decomposition into features should be done in post-processing task like in ABCD. This approach is more natural in term of sharing kernels rather than sharing features. We wish to emphasize that this can be considered as a stochastic kernel generative process as in (Jang et al. 2017).

Figure 3 illustrates gpLFM, LKM and R-ABCD (Hwang, Tong, and Choi 2016) in the plate notations. R-ABCD shares a global kernel for all time series but allocates a distinctive kernel \mathbf{C}_n for each time series. Moreover, spectral mixture kernel (Wilson and Adams 2013) is used for \mathbf{C}_n in R-ABCD prevents ones from generating explainable interpretation.

Well-definedness of gpLFM and LKM

Since the matrix \mathbf{Z} is imposed an IBP prior, the number of its columns presumably can go to infinity, thus we may have infinite kernels. We are going to answer the question whether $p(\mathbf{X} | \mathbf{Z})$ forms a well-defined probability distribution when we have infinite kernels. (Griffiths and Ghahramani 2011) gave a detailed answer on the LFM. Is this property still hold for gpLFM and LKM?

We show that the model constructions of gpLFM and LKM are well-defined. For the case of gpLFM, it is required to marginalize \mathbf{F} out of $p(\mathbf{X} | \mathbf{F}, \mathbf{Z}) p(\mathbf{F})$ in order to obtain $p(\mathbf{X} | \mathbf{Z})$. The main idea is to represent \mathbf{F} as $\text{vec}(\mathbf{F})$. Here, $\text{vec}(\cdot)$ is the vectorization. With the new representation, $p(\text{vec}(\mathbf{F}))$ becomes Gaussian, and we also reinterpret $p(\mathbf{X} | \mathbf{Z}, \mathbf{F})$ in terms of $\text{vec}(\mathbf{F})$. The marginalization of Gaussian can be done as a consequence of the above step. For the case of LKM, the likelihood $p(\mathbf{X} | \mathbf{Z})$ is straightforward, written as a multiplication of GP likelihoods. The proving technique involves performing the left-order (*lof*) form operation which orders the columns to get nonzero columns in \mathbf{Z} and justifying based on the fact that the number of nonzero columns is finite. Readers may refer our proofs for both models in Appendix .

	9 stocks		6 houses		4 currencies	
	RMSE	MNLP	RMSE	MNLP	RMSE	MNLP
Spike and Slab	10.26	2.88	11.33	6.92	151.37	3.98
GPRN	6.30	2.61	8.84	6.28	<u>117.05</u>	4.03
ABCD	8.35	2.54	7.96	<u>5.57</u>	330.00	4.50
R-ABCD	<u>4.85</u>	<u>1.89</u>	<u>3.10</u>	6.15	210.56	3.61
gpLFM	4.82	<u>1.82</u>	2.28	5.29	81.98	<u>3.44</u>
LKM	4.30	1.69	<u>3.42</u>	5.32	57.74	3.26

Table 1: RMSEs and NMLPs for each data set with corresponding methods. In most cases, our gpLFM and LKM have lower RMSEs and NMLPs compared to those of existing methods. Additional experimental results in 7 different settings are reported in the supplementary material.

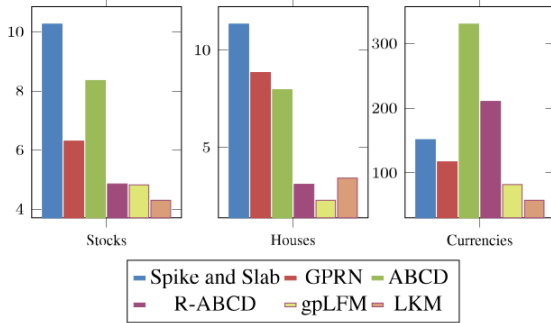


Figure 4: RMSEs for each data set (9 stocks, 6 houses, 4 currencies) with corresponding methods.

Structure Discovery

In this section, we present a search procedure to discover the structure of \mathbf{C}_k associated with the features of gpLFM or the GP kernel construction of LKM. Then, we compare the space of kernel structures produced by our approach and the compositional kernel learning (CKL) in ABCD.

Search scheme Due to the broad structure space, we design a greedy algorithm with the same spirit of (Grosse et al. 2012; Duvenaud et al. 2013; Lloyd et al. 2014). That is, we maintain a set of additive kernel structures $\{\mathcal{S}_d^{(k)} | \mathcal{S}_d^{(k)} = \prod_l \mathcal{B}_d^{(k_l)} \text{ with } \mathcal{B}_d^{(k_l)} \text{ s are base kernels, } k = 1 \dots K\}$ at a depth d . We map correspondingly $\mathcal{S}_d^{(k)}$ to the required covariances \mathbf{C}_k in our models. At the next depth, the set will recruit new additive kernels which are expanded from the elements of the set. The context-free grammar rules of the expansion are the same with CKL. However, for the case when $\mathcal{S}_d^{(k)}$ is expanded into a new kernel which is written in an additive form as $\sum_{m=1}^M \mathcal{S}_d^{(k_m)}$, we will consider this expansion as M separated expansions $\mathcal{S}_d^{(k)} \rightarrow \mathcal{S}_d^{(k_m)}$. The generated structures $\mathcal{S}_d^{(k_m)}$ will be used instead of the sum $\sum_{m=1}^M \mathcal{S}_d^{(k_m)}$. This is to make sure that the new candidate structures always satisfy the definition of $\{\mathcal{S}_d^{(k)}\}$.

Partial expansion (PE) We iteratively expand $\mathcal{S}_d^{(k)}$ and obtain a set of candidates $\{\mathcal{S}_d^{(k_1)}, \dots, \mathcal{S}_d^{(k_m)}\}$. We make a new set which is the union of the previous one excluded the selected structure $\{\mathcal{S}_d^{(k)}\}_{k=1}^K \setminus \{\mathcal{S}_d^{(i)}\}$ and the new candidate structures $\{\mathcal{S}_d^{(i_1)}, \dots, \mathcal{S}_d^{(i_m)}\}$. We run variational inference using this set to learning \mathbf{Z} and GP. Learned models will still be evaluated by BIC like in CKL. If an expanded model achieves better performance, the adaptive kernel set will keep this model. Otherwise, it rolls back to the previous one. We explore several search strategies such as full expansion (FE) where all structures in $\{\mathcal{S}_d^{(k)}\}_{k=1}^K$ are expanded together (see Appendix). We found that PE has the following advantages over alternatives: (1) it does not suffer drastic increases in structure space in each expansion, (2) it carefully assesses models by a selection criterion (BIC) and flexibly falls back to the previous model if the criterion does not select the new one, (3) it shows promising empirical results (Section). Additionally, the fewer number of kernels in PE makes us easier to initialize GP hyperparameters as well as reduce the number of restarts learning \mathbf{Z} . After learning \mathbf{Z} given a set of structures, non-active structures are removed from the additive kernel sets. We proceed to the next expansion using this updated one.

Comparison of search space in PE with gpLFM/LKM and CKL We emphasize that PE with gpLFM/LKM considers a larger number of kernel structures than those in CKL. Suppose that CKL and our search algorithm have the same found structure at a depth d . While the CKL’s structure is $\mathcal{S}_d = \mathcal{S}_d^{(1)} + \dots + \mathcal{S}_d^{(K)}$, PE represents as a set $\{\mathcal{S}_d^{(1)}, \dots, \mathcal{S}_d^{(K)}\}$. Let us examine the cardinality of kernel spaces after performing an expansion to the next depth. The procedure is to extract substructures from the current structure, then apply grammar rules on the structure. In CKL, substructures consist of all structures generated from the combinations of $\mathcal{B}_d^{(k_l)}$ in each individual $\mathcal{S}_d^{(k)}$ and ones generated by the combination of all $\mathcal{S}_d^{(k)}$. The former has $O(K \sum_l \binom{L}{l}) = O(K2^L)$ substructures where L is the largest number of base kernels in $\mathcal{S}_d^{(k)}$. The latter creates $O(\sum_k \binom{K}{k}) = O(2^K)$ combinations. When the maximum number of grammar rules per substructure is R , the total number of candidates at the depth $d+1$ is $O(RK2^L + R2^K)$.

Our approach only applies expansion on individual structure $\mathcal{S}_d^{(k)}$ via the combinations of $\mathcal{B}_d^{(k_i)}$. However, the search space still includes all the cases when substructures are extracted from a combination of $\mathcal{S}_d^{(k)}$. For instance, the generation from LIN+PER+SE to (LIN+PER) \times SE+SE in CKL is equivalent to the generation from {LIN, PER, SE} to {LIN \times SE, PER \times SE, SE} in our approach. For the case of PE, the additive kernel set will be expanded into a new one having the number of elements $R2^L + K$. With the flexible binary indications (on/off) of \mathbf{Z} , the number of all possible kernels is $O(K2^{R2^L+K})$ when all structures are visited to be expanded.

Although our search algorithm explores a much larger search space than CKL in theory, the prior over \mathbf{Z} still limits the expressiveness of our models. Moreover, our search algorithms rely on a gradient-based method where the global optimal is not guaranteed. Thus, it is not yet guaranteed to find the optimal kernel over all the possible candidates.

Experimental Results

We conduct experiments on a synthetic data set and three real world data sets. We report the analysis on synthetic data which is illustrated in Figure 1 in the supplementary material. In this section, we report the results of real-world data, then give an example of generated comparison descriptions.

Real-world time series data

Data sets We tested our algorithm on three different data sets: US stock prices, US housing markets and currency exchanges. These data sets are well-described and publicly accessible (Hwang, Tong, and Choi 2016). The US stock price data set consists of 9 stocks (GE, MSFT, XOM, PFE, C, WMT, INTC, BP, and AIG) containing 129 adjusted closes taken from the second half of 2001. The US housing market data set includes the 120-month housing prices of 6 cities (New York, Los Angeles, Chicago, Phoenix, San Diego, San Francisco) from 2004 to 2013. The currency data set includes 4 currency exchange rates from US dollar to 4 emerging markets: South African Rand (ZAR), Indonesian Rupiah (IDR), Malaysian Ringgit (MYR), and Russian Rouble (RUB). Each currency exchange time series has 132 data points.

Compare to multi-task GPs We compare multi-task GP models including ‘Spike and Slab’ model (Titsias and Lázaro-Gredilla 2011) and GP regression network (GPRN) (Wilson, Knowles, and Ghahramani 2012; Nguyen and Bonilla 2013). Root mean square error (RMSE) and Mean Negative Log Likelihood (MNLP) (Lázaro-Gredilla et al. 2010) are the used evaluation metrics in all data sets. The result in Table 1 and Figure 4 indicates that our methods significantly outperform these models. Handling real-world time series is a difficult task for these two models since the used kernels are not expressive enough (smoothing only). The expressiveness of compositional kernels plays crucial roles to fit complex data. Both gpLFM and LKM are leveraged by using compositional kernels where best structures are searched. Spike and Slab and GPRN models perform better than ABCD and R-ABCD

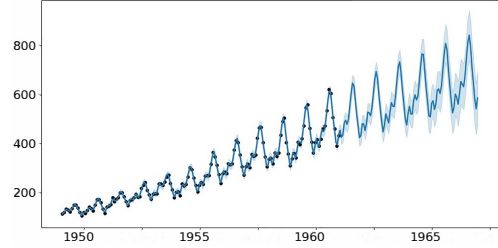


Figure 5: Posterior mean and variance of airline data set. LKM found a set of kernels including SE_1 (long lengthscale), SE_2 (short lengthscale), LIN_1 , $LIN_2 \times SE$, $LIN_3 \times WN$, $LIN_4 \times PER$, $LIN_5 \times LIN_6$. While ABCD discovered $SE_1 \times LIN_1$, $SE_2 \times LIN_2 \times PER$, and $SE_3 \times LIN_3 \times RQ$ (RQ is rational quadratic kernel). Note that our search algorithm only run after depth 2, the result reported in (Duvenaud et al. 2013) is done at depth 10. The running time of LKM is roughly 4 times faster than (Duvenaud et al. 2013).

in the currency data set where it contains highly volatile data. Although our models share some computational procedures with ABCD and R-ABCD, our models are more robust to handle different types of time series data.

Comparison of kernel composition approaches We ran ABCD on individual time series then aggregated the results to compare with our models. On these data sets, our models outperform ABCD which is known as one of the state-of-the-art GP-based regression methods on univariate time series. It proves that our belief about the correlations among multiple time series is plausible. To verify the ability of our models with the search algorithm for even a single time series, we test LKM on airline passenger data (Box and Reinsel 1976). Our method can achieve an adequately good kernel which captures all properties of data stated in (Rasmussen and Williams 2005) (includes trend and periodicity). The details of the found kernel are illustrated in Figure 5.

We then compare with R-ABCD (Hwang, Tong, and Choi 2016). Rather than making the assumption that all time series share a single global kernel, our model recognizes which structures are shared globally or partially. Quantitatively, both gpLFM and LKM show promising results in prediction tasks. They outrun R-ABCD in housing data set and currency data set while obtaining a comparable result in stock data set.

Found kernels are qualitatively good. That is, gpLFM can describe changes in multiple time series which coincide with actual real events. As an example, in the currency data set, the financial events happening September and October in 2015 (Hwang, Tong, and Choi 2016) also are discovered by our methods. The found kernels are $CW(SE, LIN)$ and $CW(SE, SE)$ where steep drops describe the sudden changes in a small window-time. Appendix contains more detailed results of the currency data set as well as another example of recognizing the US subprime mortgage crisis in house data sets.

Comparison report

By taking the advantage of the learned latent matrix \mathbf{Z} and the descriptive properties of found GP covariance structures, we generate a human-readable report containing the comparison among time series. For example, the generated text can have formats like

“ $[T_1, \dots, T_m]$ share $[description]$ ”

where the replacement of $[T_1, \dots, T_m]$ is a set of time series, $[description]$ is generated by the found GP structure. We put sample reports for housing data set and currency exchange data set in the supplementary material.

Conclusion

In this paper, we study a new perspective of multi-task GP learning where kernel structures are appropriately selected. We introduce two novel models: gpLFM which decomposes data into GP features and LKM which learns kernel decompositions from a stochastic kernel process. We further present a pragmatic search algorithm leveraging our models to explore a larger structure space than the existing algorithm. Experiments demonstrate promising performance in prediction tasks. Our proposed models also output a high-quality set of interpretable kernels which produces a comparison reports among multiple time series.

Acknowledgement

This work is supported by Basic Science Research Program through the National Research Foundation of Korea (NRF) grant funded by the the Korea government (MSIT: the Ministry of Science and ICT) (NRF- 2014R1A1A1002662) and Institute for Information and communications Technology Promotion (IITP) grant funded by the MSIT (No.2017-0-01779, a machine learning and statistical inference framework for explainable artificial intelligence).

References

- Abadi, M.; Agarwal, A.; Barham, P.; Brevdo, E.; Chen, Z.; Citro, C.; Corrado, G. S.; Davis, A.; Dean, J.; Devin, M.; Ghemawat, S.; Goodfellow, I.; Harp, A.; Irving, G.; Isard, M.; Jia, Y.; Jozefowicz, R.; Kaiser, L.; Kudlur, M.; Levenberg, J.; Mané, D.; Monga, R.; Moore, S.; Murray, D.; Olah, C.; Schuster, M.; Shlens, J.; Steiner, B.; Sutskever, I.; Talwar, K.; Tucker, P.; Vanhoucke, V.; Vasudevan, V.; Viégas, F.; Vinyals, O.; Warden, P.; Wattenberg, M.; Wicke, M.; Yu, Y.; and Zheng, X. 2015. TensorFlow: Large-scale machine learning on heterogeneous systems. Software available from tensorflow.org.
- Álvarez, M. A.; Rosasco, L.; and Lawrence, N. D. 2012. Kernels for vector-valued functions: A review. *Foundations and Trends in Machine Learning* 4(3).
- Bollerslev, T. 1986. Generalized autoregressive conditional heteroskedasticity. *Journal of Econometrics* 31(3):307 – 327.
- Bonilla, E. V.; Chai, K. M. A.; and Williams, C. K. I. 2007. Multi-task gaussian process prediction. In *NIPS*.
- Box, G.E.P., J. G., and Reinsel, G. 1976. *Time series analysis: forecasting and control*. Wiley.
- Broderick, T.; Kulis, B.; and Jordan, M. I. 2013. Mad-bayes: Map-based asymptotic derivations from bayes. In *ICML*.
- Doshi, F.; Miller, K.; Gael, J. V.; and Teh, Y. W. 2009. Variational inference for the indian buffet process. In *AISTATS*.
- Duvenaud, D.; Lloyd, J. R.; Grosse, R.; Tenenbaum, J. B.; and Ghahramani, Z. 2013. Structure discovery in nonparametric regression through compositional kernel search. In *ICML*.
- F. Engle, R. 1982. Autoregressive conditional heteroskedasticity with estimates of the variance of united kingdom inflation. 50:987–1007.
- Ghahramani, Z. 2015. Probabilistic machine learning and artificial intelligence. *Nature* 521(7553):452–459.
- Griffiths, T. L., and Ghahramani, Z. 2005. Infinite latent feature models and the indian buffet process. In *NIPS*.
- Griffiths, T. L., and Ghahramani, Z. 2011. The indian buffet process: An introduction and review. *Journal of Machine Learning Research* 12.
- Grosse, R.; Salakhutdinov, R.; Freeman, W.; and Tenenbaum, J. 2012. Exploiting compositionality to explore a large space of model structures. In *UAI*.
- Groves, T., and Rothenberg, T. 1969. A note on the expected value of an inverse matrix.
- Guarnizo, C.; Álvarez, M. A.; and Orozco, Á. Á. 2015. Indian buffet process for model selection in latent force models. In *CIARP*.
- Guarnizo, C., and Álvarez, M. A. 2015. Indian Buffet process for model selection in convolved multiple-output Gaussian processes. *ArXiv e-prints* 1503.06432.
- Hamilton, J. 1994. *Time series analysis*. Princeton, NJ: Princeton Univ. Press.
- Hwang, Y.; Tong, A.; and Choi, J. 2016. Automatic construction of nonparametric relational regression models for multiple time series. In *ICML*.
- Jang, P. A.; Loeb, A.; Davidow, M.; and Wilson, A. G. 2017. Scalable levy process priors for spectral kernel learning. In *NIPS*. 3943–3952.
- Kim, H., and Teh, Y. W. 2018. Scaling up the Automatic Statistician: Scalable structure discovery using Gaussian processes. In *AISTATS*, 575–584.
- Lázaro-Gredilla, M.; Quiñero Candela, J.; Rasmussen, C. E.; and Figueiras-Vidal, A. R. 2010. Sparse spectrum gaussian process regression. *J. Mach. Learn. Res.* 11:1865–1881.
- LeCun, Y.; Boser, B.; Denker, J. S.; Henderson, D.; Howard, R. E.; Hubbard, W.; and Jackel, L. D. 1989. Backpropagation applied to handwritten zip code recognition. *Neural Computation* 1(4):541–551.
- Lloyd, J. R.; Duvenaud, D.; Grosse, R.; Tenenbaum, J. B.; and Ghahramani, Z. 2014. Automatic construction and Natural-Language description of nonparametric regression models. In *AAAI*.
- MacKay, D. J. C. 2002. *Information Theory, Inference & Learning Algorithms*. New York, NY, USA: Cambridge University Press.
- Malkomes, G.; Schaff, C.; and Garnett, R. 2016. Bayesian optimization for automated model selection. In *NIPS*, 2892–2900.
- Matthews, A. G. d. G.; van der Wilk, M.; Nickson, T.; Fujii, K.; Boukouvalas, A.; León-Villagrà, P.; Ghahramani, Z.; and Hensman, J. 2017. GPflow: A Gaussian process library using TensorFlow. *Journal of Machine Learning Research* 18(40):1–6.
- Nguyen, T., and Bonilla, E. 2013. Efficient variational inference for gaussian process regression networks. In *AISTATS*, 472–480.
- Poon, H., and Domingos, P. M. 2011. Sum-product networks: A new deep architecture. In *Proceedings of the Conference on Uncertainty in Artificial Intelligence, UAI*, 337–346.
- Rasmussen, C. E., and Williams, C. K. I. 2005. *Gaussian Processes for Machine Learning (Adaptive Computation and Machine Learning)*. The MIT Press.
- Schaehtle, U.; Zinberg, B.; Radul, A.; Stathis, K.; and Mansinghka, V. K. 2015. Probabilistic programming with gaussian process memoization. *CoRR* abs/1512.05665.
- Schulz, E.; Tenenbaum, J.; Duvenaud, D. K.; Speekenbrink, M.; and Gershman, S. J. 2016. Probing the compositionality of intuitive functions. In *NIPS*.
- Schulz, E.; Tenenbaum, J. B.; Duvenaud, D.; Speekenbrink, M.; and Gershman, S. J. 2017. Compositional inductive biases in function learning. *Cognitive Psychology* 99(Supplement C):44 – 79.
- Titsias, M. K., and Lázaro-Gredilla, M. 2011. Spike and slab variational inference for multi-task and multiple kernel learning. In *NIPS*.
- Wainwright, M. J., and Jordan, M. I. 2008. Graphical models, exponential families, and variational inference. *Foundations and Trends in Machine Learning* 1(1-2).

Wilson, A. G., and Adams, R. P. 2013. Gaussian process kernels for pattern discovery and extrapolation. In *ICML*, 1067–1075.

Wilson, A. G.; Knowles, D. A.; and Ghahramani, Z. 2012. Gaussian process regression networks. In *ICML*.

Supplementary Material for Discovering Explainable Latent Covariance Structures for Multiple Time Series

Related Work

There are cognitive studies (Schulz et al. 2016; 2017) showing that compositional functions are intuitively preferred by human; some attempts to scale up or improve the model selection in ABCD (Kim and Teh 2018; Malkomes, Schaff, and Garnett 2016). For multiple time series, (Hwang, Tong, and Choi 2016) introduced a global *shared* information among multiple sequences and individual kernels for each kernel. Unfortunately, although the individual kernels are modeled by expressive kernels - spectral mixture kernel (Wilson and Adams 2013), they are not interpretable. We see our work as the generalization of (Hwang, Tong, and Choi 2016) where no such strong correlation assumption is posed but the relation among time series is automatically discovered by IBP matrix.

In the multi-task learning perspective, multi-task learning for GP regression has been studied extensively (Bonilla, Chai, and Williams 2007; Titsias and Lázaro-Gredilla 2011; Guarnizo, Álvarez, and Orozco 2015; Guarnizo and Álvarez 2015; Álvarez, Rosasco, and Lawrence 2012). These methods commonly share limitations that GP kernel structures are fixed or given, not having the flexibility in selecting GP kernel as in (Lloyd et al. 2014). Although gpLFM is formulated similarly to existing work (Guarnizo and Álvarez 2015; Guarnizo, Álvarez, and Orozco 2015), there is no investigation on whether the combination of IBP and GP in are well-defined. (Wilson, Knowles, and Ghahramani 2012) introduced a multi-output GP regression network (GPRN) which presents the combinations of latent GPs and weights. These weights also are encoded by Gaussian Process. Applying structure searches can be challenging due to the huge search space to cover the whole network.

Stochastic grammar for ABCD in (Schaehtle et al. 2015) is introduced where interpretable kernels are selected via a Bayesian learning over a binomial distribution imposed on the presence of kernels. It provides a sampling approach based on Venture probabilistic programming language, then there is no exact form of the likelihood function. However, it only applies single time series. While in our case, we work on multiple time series using IBP prior with an in-depth investigation of the model construction.

In terms of stochastic kernel generation, (Jang et al. 2017) proposed a Lévy kernel process where the mixture of kernels is obtained by placing a Lévy prior over the corresponding spectral density. The LKM is one of the attempts to put uncertainty on kernel constructions using IBP prior to select a set of interpretable kernels.

It is worth mentioning methods which learn complex functions including convolutional networks (LeCun et al. 1989) and sum-product networks (Poon and Domingos 2011). AND-like and OR-like operation have the intuitively similar mechanisms of multiplication and summation in compositional kernels. Beyond this similarity when using composite kernel, our work targets to study multiple complex functions where sharing features or kernels can be understanding as AND-like operation among sequences.

Base kernels and search grammar in the ABCD framework

The below table contains base kernels described in (Lloyd et al. 2014).

Base Kernels	Encoding Function	$k(x, x')$
White Noise (WN)	Uncorrelated noise	$\sigma^2 \delta(x, x')$
Constant (C)	Constant functions	σ^2
Linear (LIN)	Linear functions	$\sigma^2(x - l)(x - l')$
Squared Exponential (SE)	Smooth functions	$\sigma^2 \exp(-\frac{(x-x')^2}{2l^2})$
Periodic (PER)	Periodic functions	$\sigma^2 \frac{\exp(\frac{\cos \frac{2\pi(x-x')}{l^2}}) - I_0(\frac{1}{l^2})}{\exp(\frac{1}{l^2}) - I_0(\frac{1}{l^2})}$

Changepoint (CP) operator between two kernel functions:

$$\text{CP}(k_1, k_2) = k_1 \times \sigma + k_2 \times \bar{\sigma}.$$

where $\sigma(x, x') = \sigma(x)\sigma(x')$ with $\sigma(x) = 1/2(1 + \tanh(l-x/s))$ and $\bar{\sigma}(x, x') = (1 - \sigma(x))(1 - \sigma(x'))$. Changewindows (CW) operator between two kernel functions:

$$\text{CW}(k_1, k_2) = k_1 \times \sigma_1 \times \bar{\sigma}_2 + k_2 \times \bar{\sigma}_1 \times \sigma_2.$$

where a similar definition as in σ can be done for σ_1, σ_2 .

The language of models (or kernels) is presented by a set of rules in the grammar:

$$\begin{aligned} \mathcal{S} &\rightarrow \mathcal{S} + \mathcal{B} & \mathcal{S} &\rightarrow \mathcal{S} \times \mathcal{B} \\ \mathcal{S} &\rightarrow \text{CP}(\mathcal{S}, \mathcal{S}) & \mathcal{S} &\rightarrow \text{CW}(\mathcal{S}, \mathcal{S}) \\ \mathcal{S} &\rightarrow \mathcal{B} \end{aligned}$$

where \mathcal{S} represents any kernel subexpression, \mathcal{B} and \mathcal{B}' are base kernels (Lloyd et al. 2014).

Variational inference of gpLFM

In this section, we will give the exact form of ELBO in gpLFM as well as the parameter updates in the maximizing step of variational inference. Let us recall the form of ELBO as

$$\mathcal{L} = \mathbb{E}_{\mathbf{Z}}[\log p(\mathbf{Z})] + \mathbb{E}_{\mathbf{F}}[\log p(\mathbf{F})] + \mathbb{E}_{\mathbf{Z}, \mathbf{F}}[\log p(\mathbf{X}|\mathbf{Z}, \mathbf{F})] + H[q].$$

The first term $\mathbb{E}_{\mathbf{Z}}[\log p(\mathbf{Z})]$ can be obtained as in (Doshi et al. 2009) for either finite case (involving the Beta prior) and infinite case (constructing via stick-breaking manner). The second quantity $\mathbb{E}_{\mathbf{F}}[\log p(\mathbf{F})]$ are the summation of the followings

$$\mathbb{E}_{\mathbf{F}}[\log p(\mathbf{f}_k)] = -\frac{1}{2}(\log |2\pi \mathbf{C}_k| + \text{tr}(\mathbf{C}_k^{-1} \mathbf{S}_k) + \mathbf{m}_k^\top \mathbf{C}_k^{-1} \mathbf{m}_k),$$

with index k running from 1 to K . Next, $\mathbb{E}_{\mathbf{Z}, \mathbf{F}}[\log p(\mathbf{X}|\mathbf{Z}, \mathbf{F})]$ is factorized into N terms in the form of

$$\begin{aligned} \mathbb{E}_{\mathbf{Z}, \mathbf{F}}[\log p(\mathbf{x}_n|\mathbf{z}_n, \mathbf{F})] &= -\frac{D}{2} \\ &- \frac{1}{2\sigma_n^2} \left(\mathbf{x}_n^\top \mathbf{x}_n - 2 \sum_{k=1}^K \nu_{nk} \mathbf{m}_k^\top \mathbf{x}_n + 2 \sum_{k < k'} \nu_{nk} \nu_{nk'} \mathbf{m}_k^\top \mathbf{m}_{k'} + \sum_{k=1}^K \nu_{nk} (\text{tr}(\mathbf{S}_k) + \mathbf{m}_k^\top \mathbf{m}_k) \right). \end{aligned}$$

The evaluation of $H[q]$ consists of computing $H[q(\mathbf{Z})]$ (see (Doshi et al. 2009)) and $H[q(\mathbf{F})]$ (use the entropy of multivariate Gaussian distribution).

For the parameter updates related to \mathbf{Z} , readers may refer to (Doshi et al. 2009). For the case of \mathbf{m}_k , the typical coordinate ascent in variational inference corresponds to maximize the following function (Wainwright and Jordan 2008)

$$\begin{aligned} \log q(\mathbf{f}_k) &= \mathbb{E}_{\mathbf{Z}, \mathbf{F}_{-k}}[\log p(\mathbf{X}, \mathbf{Z}, \mathbf{F})] + c = \mathbb{E}_{\mathbf{F}_{-k}}[\log p(\mathbf{F})] + \mathbb{E}_{\mathbf{Z}, \mathbf{F}_{-k}}[\log p(\mathbf{X}|\mathbf{Z}, \mathbf{F})] + c \\ &= -\frac{1}{2} \mathbf{f}_k^\top \left(\mathbf{C}_k^{-1} + \sum_{n=1}^N \frac{\nu_{nk}}{\sigma_n^2} \mathbf{I} \right) \mathbf{f}_k + \mathbf{f}_k^\top \left(\sum_{n=1}^N \frac{\nu_{nk}}{\sigma_n^2} \left(\mathbf{x}_n - \sum_{l:l \neq k} \nu_{nl} \mathbf{m}_l \right) \right) + c, \end{aligned} \quad (6)$$

where c is constant, \mathbf{F}_{-k} is the feature matrix without \mathbf{f}_k . From (6), the closed form solution is obtained by finding the critical point of the derivative of the above quantity. It turns out that we update $\mathbf{m}_k = \mathbf{S}_k \left(\sum_{n=1}^N \frac{\nu_{nk}}{\sigma_n^2} \left(\mathbf{x}_n - \sum_{l:l \neq k} \nu_{nl} \mathbf{m}_l \right) \right)$, where \mathbf{S}_k is updated first as $\left(\mathbf{C}_k^{-1} + \sum_{n=1}^N \frac{\nu_{nk}}{\sigma_n^2} \mathbf{I} \right)^{-1}$.

Variational inference of LKM

Optimal weights for the expectation over \mathbf{Z} of the data-fit term To make it easy to follow, we restart with the bound

$$\mathbf{x}_n^\top \left(\sum_{k=1}^K w_{nk} \frac{1}{w_{nk}} \left(z_{nk} \mathbf{C}_k + \frac{\sigma_n^2}{K} \mathbf{I} \right) \right)^{-1} \mathbf{x}_n \leq \mathbf{x}_n^\top \sum_{k=1}^K w_{nk}^2 \left(z_{nk} \mathbf{C}_k + \frac{\sigma_n^2}{K} \mathbf{I} \right)^{-1} \mathbf{x}_n.$$

Here, we distribute uniformly $\sigma_n^2 \mathbf{I}$ to each $z_{nk} \mathbf{C}_k$ to make sure that $(z_{nk} \mathbf{C}_k + \frac{\sigma_n^2}{K} \mathbf{I})$ is a non-zero matrix whichever value of z_{nk} is chosen (0 or 1). Taking the expectation over \mathbf{Z} and arrange terms, we have

$$\mathbb{E}_{\mathbf{Z}} \left[\mathbf{x}_n^\top \left(\sum_{k=1}^K w_{nk} \frac{1}{w_{nk}} \left(z_{nk} \mathbf{C}_k + \frac{\sigma_n^2}{K} \mathbf{I} \right) \right)^{-1} \mathbf{x}_n \right] \leq \mathbf{x}_n^\top \sum_{k=1}^K w_{nk}^2 \mathbb{E}_{z_{nk}} \left[\left(z_{nk} \mathbf{C}_k + \frac{\sigma_n^2}{K} \mathbf{I} \right)^{-1} \right] \mathbf{x}_n.$$

Each term $\mathbb{E}_{z_{nk}} \left[\left(z_{nk} \mathbf{C}_k + \frac{\sigma_n^2}{K} \mathbf{I} \right)^{-1} \right]$ can be evaluated straightforwardly as $\left(\nu_{nk} \mathbf{C}_k + \frac{\sigma_n^2}{K} \mathbf{I} \right)^{-1} + (1 - \nu_{nk}) \frac{K}{\sigma_n^2} \mathbf{I}$. Let $a_{nk} = \mathbb{E}_{\mathbf{Z}} \left[\left(z_{nk} \mathbf{C}_k + \frac{\sigma_n^2}{K} \mathbf{I} \right)^{-1} \right]$. We set up a constraint optimization problem as follows, for each n ,

$$\min_{w_{nk}} \sum_{k=1}^K a_{nk} w_{nk}^2 \quad \text{such that} \quad \sum_{k=1}^K w_{nk} = 1, \quad w_{nk} > 0, \quad k = 1 \dots K.$$

We then obtain the Lagrange multiplier for this problem

$$L(\mathbf{w}, \lambda) = \sum_{k=1}^K a_{nk} w_{nk}^2 - \lambda \sum_{k=1}^K w_{nk}$$

The derivative solution of $\partial L / \partial w_{nk}$ is $w_{nk} = \lambda / 2a_{nk}$. Considering that the sum of all w_{nk} should be 1, we obtain

$$\lambda = \frac{1}{\frac{1}{2} \sum_{k=1}^K a_{nk}^{-1}}.$$

Finally, we get the optimal solution as

$$w_{nk} = \frac{a_{nk}^{-1}}{\sum_k a_{nk}^{-1}}.$$

Evidence Lower Bound The optimal weights retrieved from the previous section is used to construct the ELBO of LKM as follow.

$$\log p(\mathbf{X}) \geq \mathbb{E}_{\mathbf{Z}}[\log p(\mathbf{Z})] + H[q] - \underbrace{\frac{1}{2} \left(\sum_{n=1}^N \sum_{k=1}^K w_{nk}^2 a_{nk} + \log \left| 2\pi \left(\sum_{k=1}^K \nu_{nk} \mathbf{C}_k + \sigma_n^2 \mathbf{I} \right) \right| \right)}_{\mathbb{E}_{\mathbf{Z}}[\log p(\mathbf{X}|\mathbf{Z})]}$$

We can obtain $\mathbb{E}_{\mathbf{Z}}[\log p(\mathbf{Z})]$ and $H[q]$ (q in this case is just $q(\mathbf{Z})$) in a similar way with gpLFM.

Parameter updates via optimization The closed-form update for ν_{nk} in gpLFM does not hold, replacing by a gradient-based optimization on the obtained ELBO. Here, we parameterize ν_{nk} by a sigmoid function $\nu_{nk} = 1/(1 + \exp(-\xi_{nk}))$ which corresponds the canonical parameterization of the Bernoulli distribution, keeping $\nu_{nk} \in (0, 1)$. The GP hyperparameter optimization is performed along side the variational parameters.

The implementation of LKM develops on GPflow (Matthews et al. 2017) library which operates on Tensorflow computation (Abadi et al. 2015). We make the source code available at <anonymized>.

Likelihood $p(\mathbf{X}|\mathbf{Z})$ of gpLFM

This section gives the details obtaining the likelihood $p(\mathbf{X}|\mathbf{Z})$. This is a necessary step to prove the well-definedness of gpLFM.

The distribution $p(\mathbf{X}|\mathbf{Z}, \mathbf{F})$ of \mathbf{X} given \mathbf{Z}, \mathbf{F} and σ_X (WLOG we can assign all σ_n equal to σ_X) is

$$p(\mathbf{X}|\mathbf{Z}, \mathbf{F}) = (2\pi\sigma_X^2)^{-ND/2} \exp\left\{-\frac{1}{2\sigma_X^2} \text{tr}((\mathbf{X}-\mathbf{ZF})^\top (\mathbf{X}-\mathbf{ZF}))\right\}, \quad (7)$$

where $\text{tr}(\cdot)$ is the trace of matrix. Since each row \mathbf{f}_k in \mathbf{F} representing a feature is placed a GP prior with covariance kernel \mathbf{C}_k

$$p(\mathbf{f}_k) = (2\pi)^{-D/2} |\mathbf{C}_k|^{-1/2} \exp\left(-\frac{1}{2} \mathbf{f}_k^\top \mathbf{C}_k^{-1} \mathbf{f}_k\right),$$

where $|\cdot|$ denotes the determinant of matrix. Since these features are independent, the prior distribution $p(\mathbf{F})$ over \mathbf{F} is constituted from the product of $p(\mathbf{f}_k|\mathbf{C}_k)$

$$p(\mathbf{F}) = (2\pi)^{-KD/2} \prod_{k=1}^K |\mathbf{C}_k|^{-1/2} \exp\left(-\frac{1}{2} \sum_{k=1}^K \mathbf{f}_k^\top \mathbf{C}_k^{-1} \mathbf{f}_k\right). \quad (8)$$

As we mentioned in the main text, $p(\mathbf{F})$ is not truly Gaussian but the distributions of its individual rows $p(\mathbf{f}_k)$ are. To fit with the Gaussianity of $p(\mathbf{X}|\mathbf{Z}, \mathbf{F})$, we use the vectorization on matrix \mathbf{F} . The exponentiated term in (8) can be written as $\sum_{k=1}^K \mathbf{f}_k^\top \mathbf{C}_k^{-1} \mathbf{f}_k = \text{vec}(\mathbf{F}^\top)^\top \bigoplus_{k=1}^K \mathbf{C}_k^{-1} \text{vec}(\mathbf{F}^\top)$, where $\text{vec}(\cdot)$ is the vectorization which transforms a matrix into a column vector by stacking the columns of a matrix, \bigoplus is the direct sum operation of matrix. This quantity can be understood as a Gaussian distribution $p(\text{vec}(\mathbf{F}))$ and illustrated in Figure 6.

Next, we rewrite $p(\mathbf{X}|\mathbf{Z}, \mathbf{F})$ using the new representation of \mathbf{F} as $\text{vec}(\mathbf{F})$. Some algebraic properties² between trace and vectorization are applied to get the followings:

$$\begin{aligned} \text{tr}(\mathbf{X}^\top \mathbf{ZF}) &= \text{tr}(\mathbf{FX}^\top \mathbf{Z}) = \text{vec}(\mathbf{F}^\top)^\top \text{vec}(\mathbf{X}^\top \mathbf{Z}); \\ \text{tr}(\mathbf{F}^\top \mathbf{Z}^\top \mathbf{X}) &= \text{tr}(\mathbf{Z}^\top \mathbf{XF}^\top) = \text{vec}(\mathbf{X}^\top \mathbf{Z})^\top \text{vec}(\mathbf{F}^\top), \end{aligned}$$

²Cyclic permutation: $\text{tr}(\mathbf{ABC}) = \text{tr}(\mathbf{BCA}) = \text{tr}(\mathbf{CAB})$;

Trace to vectorization: $\text{tr}(\mathbf{A}^\top \mathbf{B}) = \text{vec}(\mathbf{A})^\top \text{vec}(\mathbf{B})$;

Vectorization to Kronecker product: $\text{vec}(\mathbf{ABC}) = (\mathbf{C}^\top \otimes \mathbf{A}) \text{vec}(\mathbf{B})$

$$\begin{bmatrix} \mathbf{f}_1^\top & \cdots & \mathbf{f}_K^\top \end{bmatrix} \begin{bmatrix} \mathbf{C}_1^{-1} & \mathbf{0} & \mathbf{0} \\ \mathbf{0} & \ddots & \mathbf{0} \\ \mathbf{0} & \mathbf{0} & \mathbf{C}_K^{-1} \end{bmatrix} \begin{bmatrix} \mathbf{f}_1 \\ \vdots \\ \mathbf{f}_K \end{bmatrix}$$

Figure 6: Illustration of representing $\sum_{k=1}^K \mathbf{f}_k^\top \mathbf{C}_k^{-1} \mathbf{f}_k$. The first row vector is the concatenation of \mathbf{f}_k^\top , being written as $\text{vec}(\mathbf{F}^\top)^\top$. The block matrix is a block diagonal matrix where the block at diagonal position are \mathbf{C}_k^{-1} . The last column vector is the transpose of the first row vector.

where the invariance of cyclic permutation of trace and the conversion from trace to vectorization are used respectively;

$$\begin{aligned} \text{tr}[(\mathbf{Z}\mathbf{F})^\top(\mathbf{Z}\mathbf{F})] &= \text{tr}[(\mathbf{Z}\mathbf{F})(\mathbf{Z}\mathbf{F})^\top] \\ &= \text{vec}(\mathbf{F}^\top \mathbf{Z}^\top)^\top \text{vec}(\mathbf{F}^\top \mathbf{Z}^\top) \\ &= \text{vec}(\mathbf{F}^\top)^\top (\mathbf{Z}^\top \mathbf{Z} \otimes \mathbf{I}) \text{vec}(\mathbf{F}^\top), \end{aligned}$$

where the first two '='s are done as the same as the previous derivation, then the vectorization is written in the form of Kronecker product. Note that \otimes is the Kronecker product. By using the above results and the technique of completing the square, we get the exponentiated term in $p(\mathbf{X}|\mathbf{Z}, \mathbf{F})p(\mathbf{F})$

$$\begin{aligned} p(\mathbf{X}|\mathbf{Z}, \mathbf{F})p(\mathbf{F}) &= \text{tr}\left\{\frac{1}{\sigma_X^2}(\mathbf{X} - \mathbf{Z}\mathbf{F})^\top(\mathbf{X} - \mathbf{Z}\mathbf{F})\right\} + \sum_{k=1}^K \mathbf{f}_k^\top \mathbf{C}_k^{-1} \mathbf{f}_k \\ &= \underbrace{\frac{1}{\sigma_X^2} \text{tr}(\mathbf{X}^\top \mathbf{X}) - \frac{1}{\sigma_X^2} \text{vec}(\mathbf{X}^\top \mathbf{Z})^\top \mathbf{G} \text{vec}(\mathbf{X}^\top \mathbf{Z})}_{(a)} \\ &\quad + \underbrace{(\mathbf{G} \text{vec}(\mathbf{X}^\top \mathbf{Z}) - \text{vec}(\mathbf{F}^\top))^\top \frac{\mathbf{G}^{-1}}{\sigma_X^2} (\mathbf{G} \text{vec}(\mathbf{X}^\top \mathbf{Z}) - \text{vec}(\mathbf{F}^\top))}_{(b)}, \end{aligned} \tag{9}$$

where $\mathbf{G} = (\mathbf{Z}^\top \mathbf{Z} \otimes \mathbf{I} + \sigma_X^2 \bigoplus_{k=1}^K \mathbf{C}_k^{-1})^{-1}$. Equations (7), (8) and (9) lead to the likelihood function by integrating out \mathbf{F} since (b) in (9) makes the integration tractable; only (a) left in the likelihood function $p(\mathbf{X}|\mathbf{Z})$

$$\begin{aligned} p(\mathbf{X}|\mathbf{Z}) &= \int p(\mathbf{X}|\mathbf{Z}, \mathbf{F})P(\mathbf{F})d\mathbf{F} \\ &= \frac{1}{(2\pi)^{(ND+KD)/2} \sigma_X^{ND} \prod_{k=1}^K \sqrt{|\mathbf{C}_k|}} \exp\left\{-\frac{1}{2\sigma_X^2} \text{tr}(\mathbf{X}^\top \mathbf{X}) + \frac{1}{2\sigma_X^2} \text{vec}(\mathbf{X}^\top \mathbf{Z})^\top \mathbf{G} \text{vec}(\mathbf{X}^\top \mathbf{Z})\right\} \\ &\quad \int \exp\left\{-\frac{1}{2}(\mathbf{G} \text{vec}(\mathbf{X}^\top \mathbf{Z}) - \text{vec}(\mathbf{F}^\top))^\top (\sigma_X^2 \mathbf{G})^{-1} (\mathbf{G} \text{vec}(\mathbf{X}^\top \mathbf{Z}) - \text{vec}(\mathbf{F}^\top))\right\} d\mathbf{F} \\ &= \frac{\sqrt{2\pi^{KD} |\sigma_X^2 \mathbf{G}|}}{(2\pi)^{ND/2} \sigma_X^{ND} \prod_{k=1}^K \sqrt{|\mathbf{C}_k|}} \exp\left\{-\frac{1}{2\sigma_X^2} \text{tr}(\mathbf{X}^\top \mathbf{X}) + \frac{1}{2\sigma_X^2} \text{vec}(\mathbf{X}^\top \mathbf{Z})^\top \mathbf{G} \text{vec}(\mathbf{X}^\top \mathbf{Z})\right\} \\ &= \frac{1}{(2\pi)^{ND/2} \sigma_X^{ND-KD} \sqrt{|\mathbf{I} \otimes \mathbf{Z}^\top \mathbf{Z} + \sigma_X^2 \sum_{k=1}^K \mathbf{C}_k^{-1} \otimes \Delta_k|} \prod_{k=1}^K |\mathbf{C}_k|}} \\ &\quad \exp\left\{-\frac{1}{2\sigma_X^2} \text{tr}(\mathbf{X}^\top \mathbf{X}) + \frac{1}{2\sigma_X^2} \text{vec}(\mathbf{X}^\top \mathbf{Z})^\top \mathbf{G} \text{vec}(\mathbf{X}^\top \mathbf{Z})\right\}. \end{aligned}$$

We rewrite the likelihood as follows:

$$\begin{aligned} p(\mathbf{X}|\mathbf{Z}) &= \frac{(2\pi)^{-ND/2} \sigma_X^{KD-ND}}{\sqrt{|\mathbf{Z}^\top \mathbf{Z} \otimes \mathbf{I} + \sigma_X^2 \bigoplus_{k=1}^K \mathbf{C}_k^{-1}|} \prod_{k=1}^K |\mathbf{C}_k|}} \\ &\quad \exp\left\{\frac{1}{2\sigma_X^2} [-\text{tr}(\mathbf{X}^\top \mathbf{X}) + \text{vec}(\mathbf{X}^\top \mathbf{Z})^\top \mathbf{G} \text{vec}(\mathbf{X}^\top \mathbf{Z})]\right\}. \end{aligned} \tag{10}$$

Remark on the connection to the MAP asymptotic approach Note that when observing the likelihood function is that the MAP asymptotic of (10) falls back to the same form of feature allocation $\text{tr}(\mathbf{X}^\top (\mathbf{I} - \mathbf{Z}(\mathbf{Z}^\top \mathbf{Z})^{-1} \mathbf{Z}^\top) \mathbf{X})$ presented in (Broderick, Kulis, and Jordan 2013). From (10), we have

$$\begin{aligned} p(\mathbf{X}, \mathbf{Z}) &= p(\mathbf{X}|\mathbf{Z})p(\mathbf{Z}) \\ &= \frac{(2\pi)^{-ND/2} \sigma_X^{KD-ND}}{\sqrt{|\mathbf{Z}^\top \mathbf{Z} \otimes \mathbf{I} + \sigma_X^2 \bigoplus_{k=1}^K \mathbf{C}_k^{-1}| \prod_{k=1}^K |\mathbf{C}_k|}} \exp\left\{\frac{1}{2\sigma_X^2} [-\text{tr}(\mathbf{X}^\top \mathbf{X}) + \text{vec}(\mathbf{X}^\top \mathbf{Z})^\top \mathbf{G} \text{vec}(\mathbf{X}^\top \mathbf{Z})]\right\} \\ &\times \frac{\gamma^{K_+} \exp\{\sum_{n=1}^N \frac{\gamma}{n}\}}{\prod_{h=1}^H \tilde{K}_h!} \prod_{k=1}^{K_+} \frac{(S_{N,k} - 1)!(N - S_{N,k})!}{N!}. \end{aligned}$$

When we set $\gamma := \exp(\lambda/(2\sigma_X^2))$ and take limit $\sigma_X^2 \rightarrow 0$ for the logarithm of $p(\mathbf{X}, \mathbf{Z})$, we have

$$-2\sigma_X^2 \log p(\mathbf{X}, \mathbf{Z}) \sim \text{tr}(\mathbf{X}^\top \mathbf{X}) - \text{vec}(\mathbf{X}^\top \mathbf{Z})^\top (\mathbf{Z}^\top \mathbf{Z} \otimes \mathbf{I}) \text{vec}(\mathbf{X}^\top \mathbf{Z}) + K_+ \lambda^2.$$

Here we can write $\text{vec}(\mathbf{X}^\top \mathbf{Z})^\top (\mathbf{Z}^\top \mathbf{Z} \otimes \mathbf{I})^{-1} \text{vec}(\mathbf{X}^\top \mathbf{Z}) = \text{tr}(\mathbf{X}^\top \mathbf{Z}(\mathbf{Z}^\top \mathbf{Z})^{-1} \mathbf{X})$. Now we get the same objective as the collapsed BP-means in (Broderick, Kulis, and Jordan 2013). Although our derived likelihood $p(\mathbf{X}|\mathbf{Z})$ shows a strong connection to the standard feature allocation via the asymptotic view, this asymptotic analysis has not had a clear algorithmic contribution to learn gpLFM yet.

Well-definedness of gpLFM and LKM

Proposition 1. *The likelihood of gpLFM $p(\mathbf{X}|\mathbf{Z})$ in Eq. 10 is well-defined.*

Proof. We are going to show that if the number of columns goes to infinity, the distribution in (10) is still well-defined. To validate this, we perform *lof* on \mathbf{Z} . All nonzero features are accumulated on the left, denoted as \mathbf{Z}_+ ; the rest of columns are zero vectors, denoted as \mathbf{Z}_0 . \mathbf{Z}_+ has K_+ columns, \mathbf{Z}_0 has K_0 columns and $K = K_+ + K_0$. Note that K_+ is finite. The determinant in (10) is written as

$$\begin{aligned} |\mathbf{Z}^\top \mathbf{Z} \otimes \mathbf{I} + \sigma_X^2 \bigoplus_{k=1}^K \mathbf{C}_k^{-1}| &= \begin{bmatrix} \mathbf{Z}_+^\top \mathbf{Z}_+ & 0 \\ 0 & 0 \end{bmatrix} \otimes \mathbf{I} + \sigma_X^2 \bigoplus_{k \in K_+} \mathbf{C}_k^{-1} \oplus \bigoplus_{k \in K_0} \mathbf{C}_k^{-1} \\ &= \sigma_X^{2K_0 D} \prod_{k \in K_0} |\mathbf{C}_k^{-1}| |\mathbf{Z}_+^\top \mathbf{Z}_+ \otimes \mathbf{I} + \sigma_X^2 \bigoplus_{k \in K_+} \mathbf{C}_k^{-1}|. \end{aligned} \quad (11)$$

The term $\prod_{k \in K_0} |\mathbf{C}_k^{-1}|$ will be canceled out since the existence of $\prod_{k=1}^K |\mathbf{C}_k|$ in the denominator of (10). The same can be done for $\sigma_X^{2K_0 D}$ by taking a root square first then eliminating by σ_X^{KD} . The remaining terms $\prod_{k \in K_+} |\mathbf{C}_k|$ and $\sigma_X^{K_+ D}$ are finite. Also, the term containing \mathbf{Z} in the exponentiated expression of (10) is written as

$$\text{vec}(\mathbf{X}^\top \mathbf{Z})^\top \mathbf{G} \text{vec}(\mathbf{X}^\top \mathbf{Z}) = \text{vec}(\mathbf{X}^\top \mathbf{Z}_+)^\top (\mathbf{Z}_+^\top \mathbf{Z}_+ \otimes \mathbf{I} + \sigma_X^2 \bigoplus_{k \in K_+} \mathbf{C}_k^{-1})^{-1} \text{vec}(\mathbf{X}^\top \mathbf{Z}_+) \quad (12)$$

is finite. □

Proposition 2. *The likelihood of LKM is well-defined.*

Proof. In the case of LKM, the likelihood can be easily obtained since there is no participation of latent feature variables

$$p(\mathbf{X}|\mathbf{Z}) = \prod_{n=1}^N p(\mathbf{x}_n|\mathbf{z}_n).$$

Analogously, the *lof* operator is applied on \mathbf{Z} to get \mathbf{Z}_+ . Each row in \mathbf{Z}_+ is used to generate kernel $\mathbf{D}_n = \sum_{z_{nk} \in \mathbf{Z}_+} z_{nk} \mathbf{C}_k + \sigma_n^2 \mathbf{I}$ which is now the finite sum of covariances kernels \mathbf{C}_k . Thus, each multivariate Gaussian likelihood $p(\mathbf{x}_n|\mathbf{z}_n)$ has a well-defined covariance. Finally, we can conclude that $p(\mathbf{X}|\mathbf{Z})$ is well-defined. □

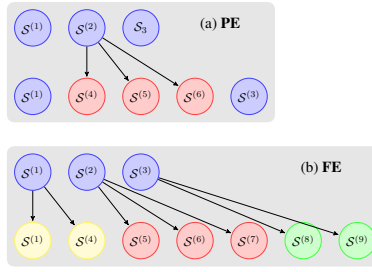


Figure 7: Structure search strategies. (a) Partial expansion (PE). (b) Full expansion (FE).

	3 stocks	6 stocks	9 stocks	2 houses	4 houses	6 houses	4 currencies
Spike and Slab	1.80	2.81	10.26	13.95	8.59	11.33	151.37
GPRN	0.49	3.76	6.30	12.96	11.07	8.84	<u>117.05</u>
ABCD	0.40	3.69	8.35	6.58	5.84	7.96	330.00
R-ABCD	<u>0.38</u>	1.22	<u>4.85</u>	<u>2.75</u>	<u>2.22</u>	<u>3.10</u>	210.56
gpLFM	0.36	<u>1.47</u>	<u>4.82</u>	2.15	2.08	2.28	81.98
LKM	<u>0.38</u>	1.69	4.30	<u>2.62</u>	2.54	3.42	57.74
FE-gpLFM	0.35	1.84	6.35	5.07	4.87	7.30	59.40
FE-LKM	0.36	1.70	4.24	4.46	3.97	6.73	<u>100.59</u>

Table 3: RMSEs on all data sets with corresponding methods. FE-gpLFM and FE-LKM are the experiment settings running in FE mode.

Synthetic data

Generating kernel	Found kernel
LIN+SE	SE+LIN+SE×LIN
LIN+LIN×SE	SE + SE
LIN+LIN×SE+PER	SE + LIN + SE + LIN×LIN + SE×PER

Table 2: Comparing the true generated kernel with the found structure

We generate synthetic three time-series according to several chosen kernels to verify our kernel selection algorithm. Each time series consists of 200 data points, generated from different kernels (see Table 2).

Although the generated data seems similar in terms of global shapes, the data has clear differences in terms of local structures. The first column of Figure 1 show the three generated time series. It is easy to notice that all time series share trending shapes with smoothing caused by LIN and SE kernels. However, the first time series has more LIN trending component than the second. In addition, PER kernel is one of the components playing the role of creating the periodicity in the third time series.

The decomposition from this synthetic data can be visually seen in Figure 1, and discovered kernels are in Table 2. Although the synthetic data shared the LIN structure, it looks like having smoothness more than having a clear LIN trending. The discovered kernel from the first time series contains the LIN structure but is dominant by the smoothness of global structures among three times series. One of the interesting observations is that the gpLFM can distinguish the PER kernel of the third time series in form of the product with SE.

Full expansion (FE)

Every structure in the additive kernel set is expanded together. The generated structures will be unified into a single set (see Fig. 7 for comparison FE and PE). The model comparison is done between search depths.

We report the additional result of our models running on FE mode in Table 3.

Comparison report

Subprime Mortgage in US house data The subprime mortgage happened around 2007 and dropped until 2009. The bold texts in the following report roughly describe this event.

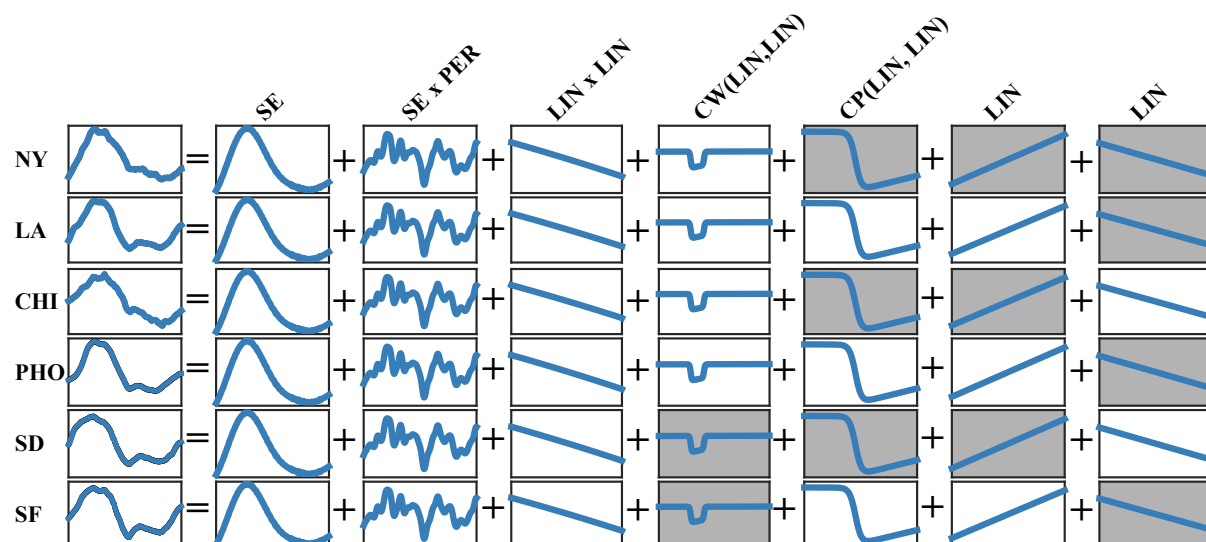


Figure 8: The decomposition of housing prices in six cities: New York (NY), Los Angeles (LA), Chicago (CHI), Phoenix (PHO), San Diego (SD), San Francisco (SF).

- NY and LA and CHI and PHO and SD and SF share the following properties
 - ▷ This component is a smooth function with a typical lengthscale of 1.8 years
- NY and LA and CHI and PHO and SD and SF share the following properties
 - ▷ This component is very approximately periodic with a period of 153.0 years. Across periods the shape of this function varies smoothly with a typical lengthscale of 3.4 months. Since this lengthscale is small relative to the period this component may more closely resemble a non-periodic smooth function
- NY and LA and CHI and PHO and SD and SF share the following properties
 - ▷ This component is a quadratic polynomial
- NY and LA and CHI and PHO share the following properties
 - ▷ This component is linearly decreasing. This component applies until **Oct. 2006** and from **Jan. 2008** onwards
- LA and PHO and SF share the following properties
 - ▷ This component is linearly increasing. This component applies until Jun 2008
- LA and PHO and SF share the following properties
 - ▷ This component is linearly increasing
- CHI and SD share the following properties
 - ▷ This component is linearly decreasing

Currency exchange of emerging markets We bring up the report for four currencies (South African Rand, Indonesian Rupiah, Malaysian Ringgit, Russian Rouble) as an example

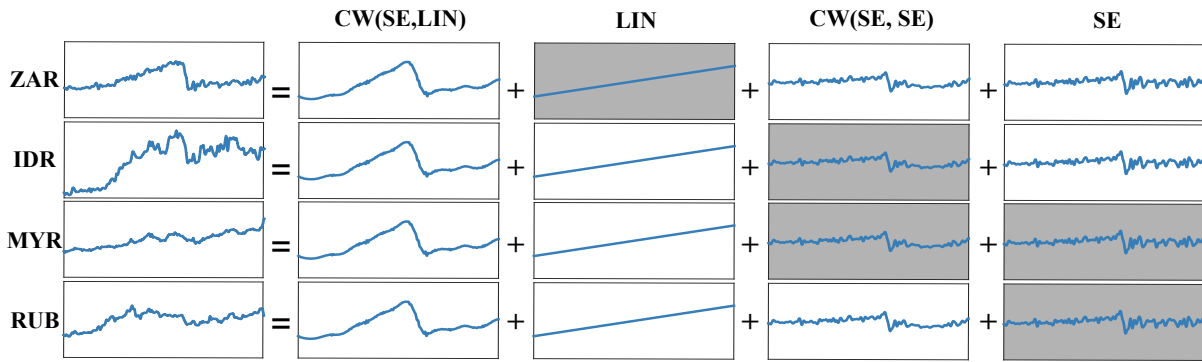


Figure 9: The decomposition of four currencies: South African Rand (ZAR), Indonesian Rupiah (IDR), Malaysian Ringgit (MYR), Russian Rouble (RUB). The shaded ones are inactive components.

- South African Rand and Indonesian Rupiah and Malaysian Ringgit and Russian Rouble share the following properties
 - ▷ This component is a smooth function with a typical lengthscale of 6.4 days. This component applies until **Sep. 15th 2015** and from **Sep. 17th 2015** onwards.
- Indonesian Rupiah and Malaysian Ringgit and Russian Rouble share the following properties
 - ▷ This component is linearly increasing.
- South African Rand and Russian Rouble share the following properties
 - ▷ This component is a smooth function with a typical lengthscale of 29.6 hours. This component applies until **Oct. 22nd 2015** and from **Nov. 10th 2015** onwards.
- South African Rand and Indonesian Rupiah share the following properties
 - ▷ This component is a smooth function with a typical lengthscale of 28.1 hours.